CRYSTAL GROWTH & DESIGN
2009
VOL. 9, NO. 5
2354–2362

O−H···N Heterosynthon: A Robust Supramolecular Unit For Crystal Engineering

Mujeeb Khan, Volker Enkelmann, and Gunther Brunklaus*

Max-Planck-Institut für Polymerforschung, Postfach 3148, D-55021 Mainz, Germany

Received November 11, 2008; Revised Manuscript Received February 19, 2009

ABSTRACT: To explore the robust nature of template resorcinols in organic solid-state reactions, a series of mono- and dipyridines were cocrystallized with different substituted resorcinols. The organizational consequences of hydrogen-bonds in the hydroxyl···pyridine heterosynthon in the presence of competitive hydrogen-bonding functional groups are elucidated. C−O bond flexibility, steric hindrance, and formation of undesired intramolecular hydrogen bonds have strongly affected the ability of the template for a parallel alignment of olefins. Finally, structural changes that occurred at a molecular level during [2 + 2] photodimerization of the complex of 1,4-bis[(*E*)-2-(4-pyridyl)ethenyl]-2-fluorobenzene (bpef) with 2,4-dihydroxy-benzaldehyde were studied in detail by performing a rather rare single-crystal-to-single-crystal photoirradiation.

1. Introduction

Crystal engineering comprises an understanding of intermolecular interactions that govern crystal packing, thus allowing the design of solids with tailored physical and chemical properties.[1−5] Indeed, an organic crystal can be regarded as an ultimate supermolecule (that is not only assembled via molecular recognition but also stabilized by rather weak, noncovalent interactions).[6,7] In recent work, great efforts have been put onto selective control or modification of reactant compounds yielding rationally designed crystal lattices.[8−10] A prominent example is given by the [2 + 2] photodimerization that has provided a large variety of compounds.[11−15] To steer olefins to react, researchers employed attractive intermolecular forces such as halogen−halogen[16,17] interactions as well as others, yielding molecules that may be difficult to achieve in solutions, such as donor−acceptor interactions[18] and hydrogen bonds.[19]

Recently, both the strength and directionality of hydrogen bonds of resorcinol have been exploited to enforce topochemical alignment of olefins in the solid state to allow for a selective [2 + 2] photoreaction.[20] A thorough understanding of supramolecular synthons (resorcinol−pyridine, O−H···N) such as their preferred geometries, competitive hydrogen bonds, strength, and recognition pattern is a prerequisite for rational design and supramolecular synthesis of novel cocrystals.[21−23] Two distinct categories of synthons are known: so-called supramolecular homosynthons, composed of self-complementary functional groups, e.g., carboxylic acid dimer,[24] and supramolecular heterosynthons,[23c,24] which are composed of different but complementary functional groups. The latter category includes hydroxyl···pyridine,[20a] hydroxyl···amine,[25] acid···pyridine,[26] and acid···amide[27] supramolecular synthons. Studies suggest that some supramolecular heterosynthons are strongly favored over related supramolecular homosynthons.[23−27] It has already been established that resorcinol, when cocrystallized with pyridine, largely forms hydroxyl···pyridine supramolecular heterosynthons.[20a] In some cases, however, the respective heterosynthons do not have the favorable orientation (ring formation, with parallel arrangement of double bonds separated at 4 Å) that is required for topochemical reactions.[28]

In this contribution, we discuss organizational consequences of hydrogen bonds within hydroxyl···pyridine heterosynthons in the presence of competitive hydrogen-bonding functional groups. To explore the robustness of such hydroxyl−pyridyl heterosynthons, we cocrystallized differently substituted resorcinols with mono- and dipyridines and determined their crystal structures. One of the supramolecular heterosynthon sustained in a favorable orientation, as shown in Scheme 1, was picked for single-crystal-to-single-crystal photodimerization, thus yielding detailed insights into intermediate states of the reaction at an atomic level. Different complementary techniques such as atomic force microscopy (AFM),[29] vibrational spectroscopy,[30] X-ray diffraction[31] and solid-state NMR[32] have been successfully applied to reveal the respective reaction mechanism, but each method has certain limitations. Because AFM is primarily sensitive to surfaces, no direct structural information can be obtained; although vibrational spectroscopy (infrared and Raman) can be indeed applied to monitor the topochemical nature of organic solid-state reactions, no conformational details of intermediate states can be obtained.

Scheme 1. Reaction Scheme for the Single-Crystal-to-Single-Crystal (SCSC) [2 + 2] Photo-Dimerization of 2,4-Dihydroxy-benzaldehyde and 1,4-Bis[(*E*)-2-(4-pyridyl)-ethenyl]-2-fluorobenzene (bpef)

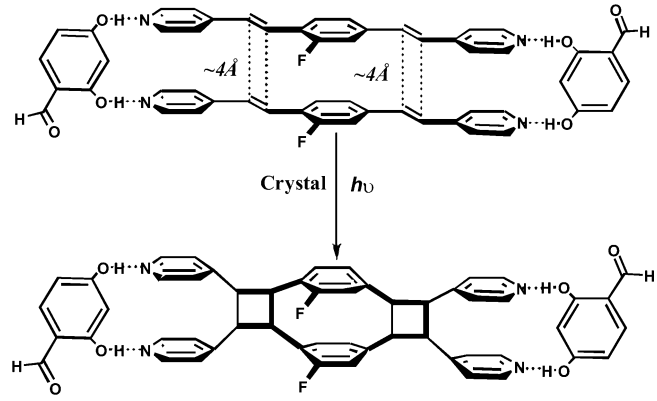

In principle, X-ray crystallography is the method of choice to study photodimerization reactions within single crystals. Upon broadband irradiation, however, crystals tend to disintegrate into microcrystalline particles as the dimerization proceeds, rendering X-ray analysis of resulting products rather difficult. This can be overcome[31a,33] when photoactive crystals are irradiated by light for which they have low absorptivity so that the intensity

* Corresponding author. E-mail: brunklaus@mpip-mainz.mpg.de.

10.1021/cg801249b CCC: $40.75
Published on Web 03/23/2009

of the light will be rather evenly distributed throughout the bulk crystal, leading to homogeneous and/or less-strained products.

2. Experimental Section

2.1. General Details. All reagents and starting materials were obtained from commercials sources and used as received. Melting points were determined at a heating rate of 5 K/minute. Solution proton NMR spectra were recorded on at 250.1 MHz, where the residual ^{1}H solvent peak was used as an internal standard ($CHCl_3$: ^{1}H, δ 7.24 ppm). UV−vis spectra were recorded on spectrophotometer (dichloromethane as solvent); mass spectra were obtained using at 70 eV. Preparative irradiations for single crystals of the monomer complex of bpef were performed with a 450 W Xenon lamp. All X-ray structures were recorded on a Kccd diffractometer with graphite-monochromated Mo Kα radiation. Lattice parameters were obtained by least-squares fits to scattering angles of reflections observed in several prescans. The intensity data collection was performed by ϕ and ω scans; raw data were corrected for Lorentz and polarization effects. The structures were solved by direct methods and refined by full matrix least-squares analyses with anisotropic temperature factors for all atoms except H. Positions of the acidic H atoms were found in difference Fourier synthesis. All other H-atoms were calculated using known molecular geometries and refined in the riding mode with fixed isotropic temperature factors. Empirical absorption corrections were applied to the data. No attempt was made to refine the occupancy factors in the disordered structures (bpef with 4-bromo-resorcinol and bpef with 2,4-dihydroxy-benzaldehyde). These were set to 50% for the two different orientations of 1,4-bis[(*E*)-2-(4-pyridyl)ethenyl]-2-fluorobenzene (bpef).

2.2. Preparations of Photoreactive Conjugated Dipyridines. All photoreactive dipyridines were prepared in the same manner by reaction of dibromobenzene,[34] ~1.25 equiv. of 4-vinylpyridine per aromatic bromine substituent, and catalytic amounts (ca. 10 mol %) of triphenylphosphine palladium dichloride in dry Et_3N at 100 °C under N_2. A representative procedure is reported here for the preparation of 1,4-bis[(E)-2-(4-pyridyl) ethenyl]-2-fluorobenzene (bpef). A mixture of 1,4-dibromo-2-fluorobenzene (0.507 g, 2 mmol), 4-vinylpyridine (0.525 g, 5 mmol), and triphenylphosphine palladium dichloride (0.140 g, 0.2 mmol) was placed in a nitrogen-purged Schlenk tube. About 1 mL dry triethylamine was added, the tube sealed, and the mixture heated to 100 °C under stirring for 3 days. After cooling, the solid dark mass was dissolved in about 200 mL of dichloromethane and extracted thoroughly with 150 mL of water three times. The residual organic phase was dried with $MgSO_4$, concentrated in vacuo, and chromatographed over silica gel using THF and low-boiling petrol ether in a 3:1 ratio. Traces of unreacted 4-vinylpyridine eluted first, followed by bpef as a dark yellow band. Evaporation to dryness followed by recrystallization from ethanol and water affording pure 0.411 g (68% yield) of bpef as yellow microcrystalline solid. ^{1}H NMR: δ 8.60 (D, 4H, Py, N=CH, J = 6 Hz); 7.61 (D, 1H, Ar, *ipso*-CH, J = 7.89 Hz); 7.46 (D, 1H, Py-CH=CH, J = 16.42 Hz); 7.36 (D, 4H, Py, *ipso*-CH, J = 5.69 Hz); 7.30 (D, 1H, Ar, *ipso*-CH, J = 7.59 Hz); 7.20 (S, 1H, Ar, *ipso*-CH); 7.15 (D, 1H, Py-CH=CH, J = 16.42 Hz); 7.06 (D, 2H, Ar−CH=CH, J = 16.42 Hz). EI-MS: m/z 302.6 (M^+). M.p.: 225.8−226.7 °C.

2.3. 2,6-Bis[(*E*)-2-(4-pyridyl)ethenyl]naphthalene (bpen). Yield: 48%, M.p.: 253 °C, EI-MS: m/z 334.4 (M^+). ^{1}H NMR: δ 8.60 (D, 4H, Py, N=CH, J = 6 Hz); 7.87 (S, 2H, Ar, *ipso*-CH,); 7.91 (D, 2H, Ar, *ipso*-CH, J = 11.39 Hz); 7.76 (D, 2H, Ar, *ipso*-CH-C=CH, J = 8.53 Hz); 7.48 (D, 2H, Ar−CH=CH, J = 16.43 Hz); 7.41 (D, 4H, Py, *ipso*-CH, J = 6.32); 7.17 (D, 2H, Py-CH=CH, J = 16.42 Hz).

2.4. Crystal Preparation. All cocrystals presented in this work were synthesized by slow evaporation of solvent or mixture of solvents at room temperature in test tubes. As an example, the cocrystallization of the complex of 1,4-bis[(*E*)-2-(4-pyridyl)ethenyl]-2-fluorobenzene (bpef) with 2,4-dihydroxy-benzaldehyde is given here: to a mixture of 5 mg (0.0165 mmol) of bpef and 2.27 mg (0.0165 mmol) of 2,4-dihydroxy-benzaldehyde (in equimolar ratio) was added a mixture of 5 mL of acetone and 5 mL of toluene. The resulting solution was heated slowly and left at room temperature for slow evaporation. After two days, dark yellow, needlelike crystals were formed. Cocrystallizations of all other complexes were performed similarly using suitable solvents (see the Supporting Information).

Table 1. List of "Reliable" and "Occasional" Hydrogen-Bonding Donors and Acceptors

type	functional group involved
reliable donors	−OH, −NH_2, −NHR, −$CONH_2$, −CONHR, −COOH
occasional donors	−COH, −XH, −SH, −CH
reliable acceptors	−COOH, −CONHCO−, −NHCONH−, −CON, −OH.
occasional acceptors	−O, −NO_2, −CN, −CO, −COOR, N<, −Cl

3. Results and Discussions

3.1. Hydrogen-Bonding Mediated Self-Assembly. Hydrogen-bonding has emerged as one of the most powerful tools among the directional, intermolecular interactions in noncovalent synthesis that mediate supramolecular assembly. From a detailed inspection of reported crystal structures, various rules to predict hydrogen-bonding arrangements in single- and two-component crystals were derived.[35,36] Nevertheless, there remains a rather strong need for hydrogen-bonding motifs that can direct the formation of predictable and ordered solid-state structures tolerating changes in both the shape and size of the spacer. The discovery of such persistent hydrogen-bonding motifs would not only allow a more reliable prediction of solid structures but also facilitates a rational construction of materials with controlled positioning of key functional groups. Etter et al.[37] applied graph theory for classifying and symbolically representing different types of hydrogen bonds that can be formed and proposed certain rules that govern hydrogen bonding in solids. Distinguishing "reliable" and "occasional" hydrogen-bond donors and acceptors (see Table 1),[37] three prominent, rather general rules were devised, which indeed apply well to small organic molecules:

(i) All (or as many as possible) good proton donors and acceptors are used in hydrogen-bonding.

(ii) If six-membered ring intramolecular hydrogen bonds can form, they will usually do so in preference to intermolecular hydrogen bonds.

(iii) The best proton donors and acceptors remaining after intramolecular hydrogen bond formation will form intermolecular hydrogen bonds.

A major challenge[38] regarding the molecular conformation of photoreactive, conjugated molecules is the control of required

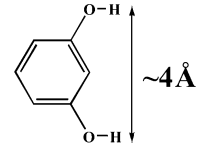

Figure 1. Approximately 4 Å distance between two hydroxyl groups of resorcinol.

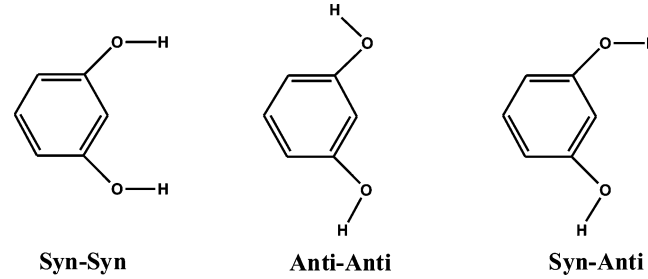

Figure 2. Three different possible hydroxyl-conformations of resorcinol with respect to the phenyl ring.[28]

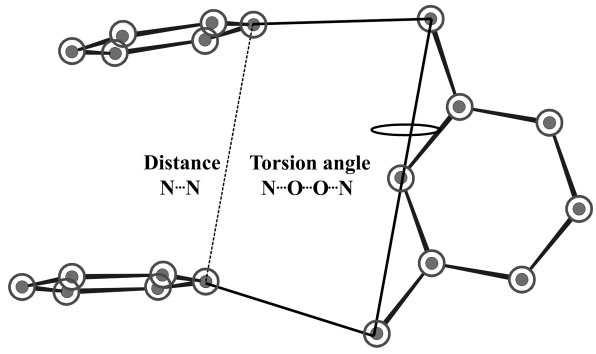

Figure 3. Hydrogen-bonding geometry of resorcinol illustrating the dependence of the N−N distance on the respective N···O···O···N torsion angle.

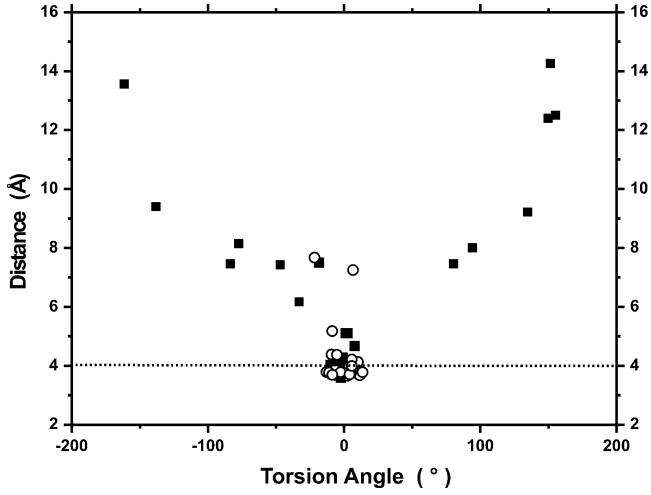

Figure 4. Plot of the observed N−N distances dependent on the N···O···O···N torsion angle. Closed circles represent literature data[41] and open circles represent data obtained in this work.

relative distances of less than 4 Å between the reactants. This can be achieved either by using a molecule that can be self-assembled to provide a desired functionality, e.g., steering the molecules into favorable orientation, or by a molecule, which itself has a desired functionality to achieve the necessary preorganization of photoreactive molecules. Though single molecules that may incorporate suitable functionality can be effective for the preparation of tailored supramolecular structures, another potentially even more powerful strategy for the design of structures comprises a combination of molecules instead. According to Lauher et al.,[38] hydroxyl groups coupled to a pyridine hydrogen-bond acceptor constitute a useful heterosynthon for the design of molecular networks. Recently, resorcinol has been used for selective preorientation of photodimerizable conjugated pyridines,[20a] because it has two hydroxyl groups at a distance of ∼4 Å (see Figure 1). Indeed, as proposed by Etter,[36] resorcinol is among the so-called "reliable" hydrogen-bonding donors. Hence, the association of the hydrogen-bond donor resorcinol and photoactive, hydrogen-bond acceptor molecules seems to provide a suitable approach to control molecular orientation and spacing of constituent molecules in photodimerization reactions. But often, the anticipated hydrogen-bonding pattern does not occur, e.g., because of the presence of multiple hydrogen-bonding sites, steric overcrowding, or competing dipolar and ionic forces. Here, in particular, it is evaluated how a hydrogen-bonding pattern adjusts to the presence of such perturbations.

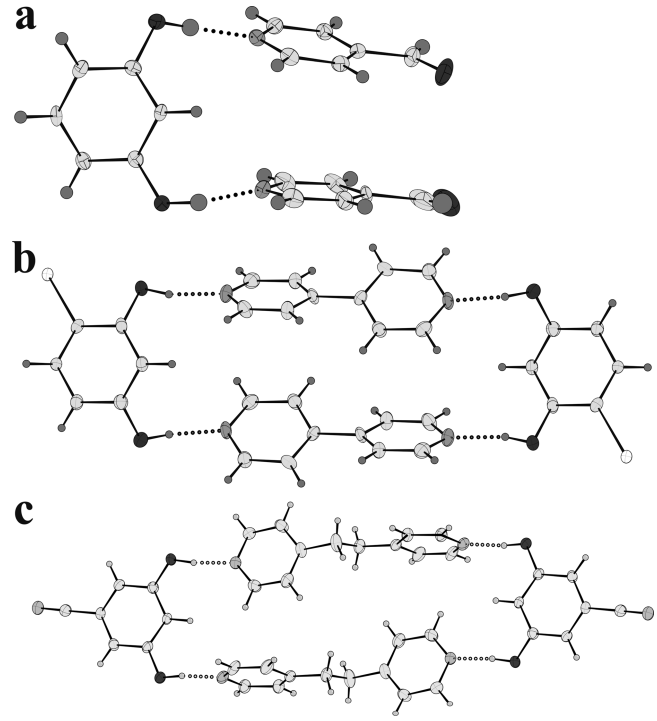

Figure 5. Two-component adducts formed by different resorcinols and monopyridines: (a) 1:1 supramolecular heterosynthon of resorcinol with 4-pyridine-carboxaldehyde; (b) 4-bromo-resorcinol and 4,4-dipyridine; and (c) 3,5-dihydroxy-benzonitrile and 1,2-bis(4-pyridyl)ethane (more examples are provided in the Supporting Information).

Cocrystals are ideally suited to study competition among supramolecular heterosynthons,[36] which are either obtained from solutions containing more than one molecular species or derived by intimately mixing or grinding two solids. Cocrystal formation is rather important in topochemical reactions, where sufficient preorientation of the reactants is required. This can be achieved by using simple organic molecules with desired functionality. Indeed, as stated earlier, the crystal structure is often a compromise among interactions of varying strengths, directionalities, and distance-dependent properties. To investigate the robustness or ability of the hydroxyl-pyridyl supramolecular heterosynthon in a variety of situations, a number of cocrystals were prepared from different substituted resorcinols and rather simple mono- or dipyridines.

3.2. O−H Group Conformations of Resorcinol. Because of the possibility of free rotation along the C−O bond, the hydrogen-bonding geometry of resorcinol is rather flexible. Three different stable conformations of the OH groups with respect to the phenyl rings are possible (see Figure 2).[28,40] When two pyridines are hydrogen-bonded to a resorcinol molecule, the distance of the N-atoms of the adjacent pyridyl rings can be described as a function of the torsion angle N···O···O···N (see Figure 3). It can be expected that this distance is smallest at a torsion angle of 0°. In this geometry, the pyridyl rings are eclipsed. In Figure 4, the distance between N-atoms is plotted as a function of the torsion angle defined in Figure 3 (closed symbols represent data taken from the literature (Cambridge Structural Database, CSD)[41] while open circles reflects data from this work). As predicted, N−N distances in the vicinity of 4 Å are only observed in a small section of this map, i.e., in an angular range of approximately −10 to 10°. It can also be seen that the majority of structures considered in our work fall in this range. This demonstrates that resorcinol indeed can be successfully employed as a template for photoreactive molecules.

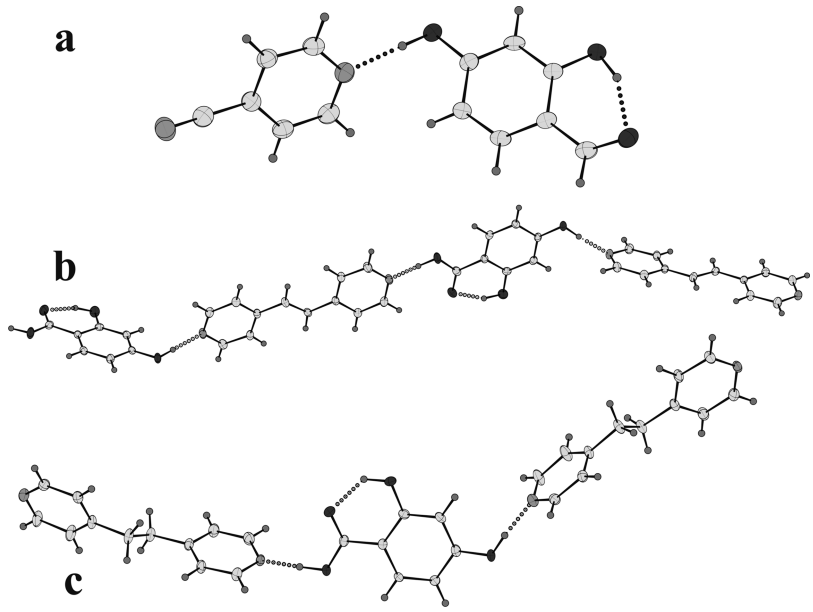

Figure 6. Cocrystallization of different substituted resorcinols with mono- or dipyridines: (a) discrete single-point molecular recognition between 2,4-dihydroxy-benzaldehyde and 4-cyano-pyridine; (b) infinite two-point molecular recognition between 2,4-dihydroxy-benzoic acid and 1,2-bis(4-pyridyl)ethylene; and (c) 2,4-dihydroxy-benzoic acid and 1,2-di-(4-pyridyl)ethane (more examples are provided in the Supporting Information).

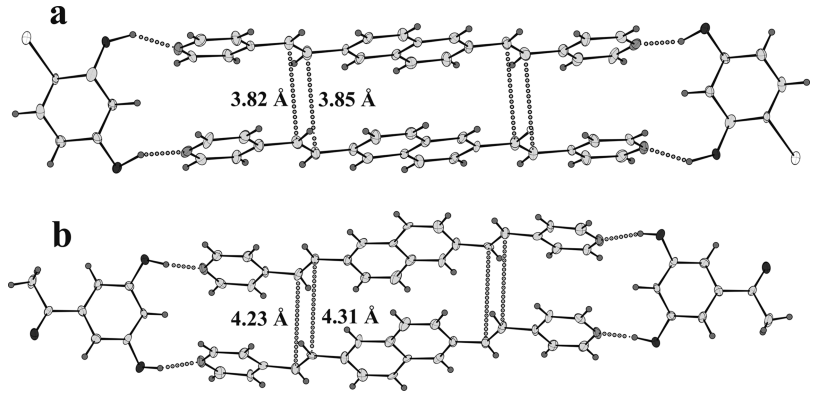

Figure 7. Complex formation of 2,6-bis[(*E*)-2-(4-pyridyl)ethenyl]naphthalene (bpen) with (a) 4-bromo-resorcinol and (b) 3,5-dihydroxy-acetophenone.

3.3. Cocrystallization of Resorcinol with Mono- or Dipyridines Leading to the Desired Structures. Figure 5 displays three examples, where the desired structures with ∼4 Å spacing were obtained by cocrystallization of resorcinols with mono- or dipyridines. A discrete two point molecular recognition, e.g., due to intermolecular hydrogen bonds between hydroxyl hydrogen and pyridyl nitrogen (OH···N) is common among all these crystal structures, orienting the pyridine molecules parallel to each other. The pyridyl rings are further stabilized by $\pi-\pi$ interactions at a distance of around 4 Å relative to each other. This type of intermolecular hydrogen-bonding facilitates the formation of centrosymmetric supramolecular adducts if dipyridines are used (see Figure 5b),[39] and is the most favorable kind of hydrogen-bonding pattern for the rational design of photoreactive molecules. Other hydrogen-bonding active functional groups, like aldehyde and nitrile groups, which are also present in these crystal structures, potentially could interfere with the desired intermolecular hydrogen-bonding, but they are rather far away from the hydrogen-bonding donor hydroxyl group. In addition, the pyridyl nitrogen is a better (and hence favored) hydrogen-bonding acceptor than carbonyl and nitrile groups.[36]

3.4. Cocrystallization of Resorcinol with Mono- Or Dipyridines Leading to Rather Undesired Structures. Hydrogen-bonding patterns frequently involve many types of hydrogen bonds with multiple, intertwined hydrogen-bonding networks, particularly in the presence of other competitive hydrogen-bonding functional groups. To test both the selectivity and preferences of the O−H···N hydrogen bond in the presence of other hydrogen-bonding active moieties, we cocrystallized substituted resorcinols containing an additional hydrogen-bonding donor functionality other than hydroxyl groups with pyridines. The crystal structure of 1:1 cocrystals of 2,4-dihydroxy-benzaldehyde and 4-cyano-pyridine (see Figure 6a) reveals that the presence of carbonyl units next to hydroxyl groups has led to a preferred six-membered ring of intramolecular hydrogen bonds.[36] Hence, only one hydroxyl group is involved in the desired intermolecular hydrogen-bonding with pyridine. The corresponding crystal structures of 1:1 adducts of 2,4-dihydroxy-benzoic acid with 1,2-di-(4-pyridyl)ethylene and 1,2-di-(4-pyridyl)ethane, respectively, are given in structures b and c in Figure 6. There are six hydrogen-bonding donors and six hydrogen-bonding acceptors present in each of these structures, but the selectivity of these hydrogen bonding motifs

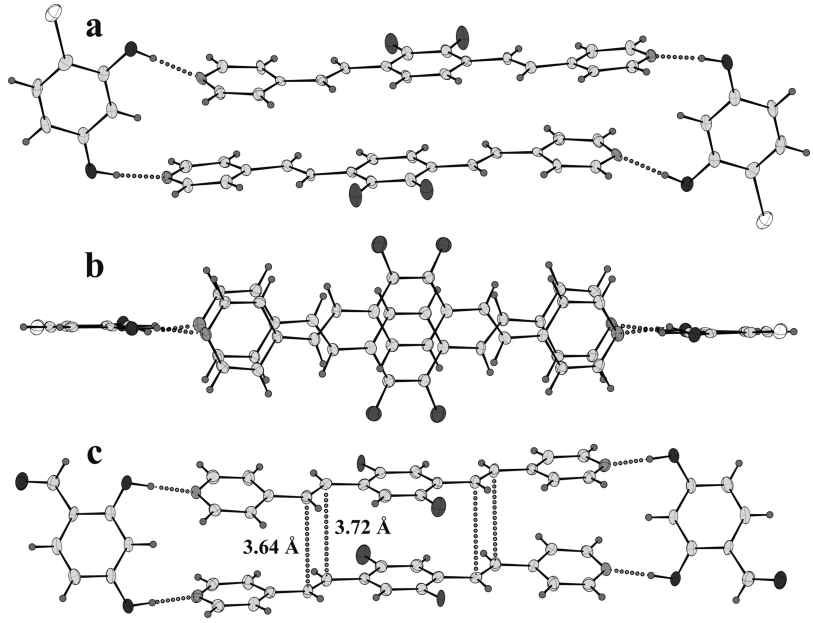

Figure 8. Crystal structure projection of the cocrystals of 1,4-bis[(*E*)-2-(4-pyridyl) ethenyl]-2-fluorobenzene (bpef) with 4-bromo-resorcinol; (b) identical complex, shown in a different projection; (c) complex formation of bpef with 2,4-dihydroxy-benzaldehyde.

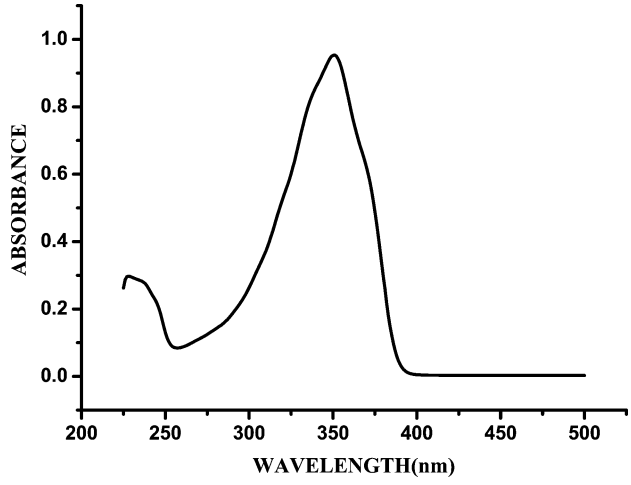

Figure 9. UV−vis absorption spectrum of 1,4-bis[(*E*)-2-(4-pyridyl)ethenyl]-2-fluoro-benzene (bpef).

are rather different. Altogether, three types of H-bonds were observed: two intermolecular hydrogen bonds among pyridyl nitrogen and hydroxyl hydrogen, as well as pyridyl nitrogen and carboxyl hydrogen yielding an infinite one-dimensional chain rather than discrete, zero-dimensional, four-point molecular recognition assembly. The third motif is the most favored six-membered ring obtained via intramolecular hydrogen bonds between hydroxyl groups and carbonyl oxygens.

Indeed, the ability of resorcinol to assemble with 1,2-bis(4-pyridyl)ethane, yielding an infinite 1D array (see the Supporting Information) where the spacer adopts a divergent conformation that prevents stacking of dipyridine, has already been reported.[28] Therefore, to achieve the desired 0D assembly,[20] substituted resorcinols that possess the ability to possibly block a formation of H-bonded chains, such as 4-chloro-resorcinol and 4,6-dichloro-resorcinol, were used. The main reason for the observed chain formation in flexible 1,2-bis(4-pyridyl)ethane, even in the absence of an undesired intramolecular hydrogen bond, is the presence of bulky CH_2—CH_2 linkages that preclude stacking of dipyridines. As described above, a formation of chainlike structures is facilitated by free rotation of the C−O bond in resorcinol, thus an O−H···N heterosynthon may be formed avoiding steric hindrance. However, because of this rotation, the two O−H bonds in resorcinol are not necessarily oriented parallel to each other.

3.5. Molecular Recognition of Photoreactive Conjugated Dipyridines. Clearly, by choosing appropriate resorcinols, a rational design of photoreactive crystals can be achieved. To extend the approach of solid-state molecular assembly in the presence of competitive hydrogen-bonding active moieties, we synthesized different conjugated dipyridines consisting of two hydrogen-bond acceptors and photoactive vinylic double bonds separated by an aromatic moiety, e.g., 2,6-bis[(*E*)-2-(4-pyridyl)ethenyl]naphthalene (bpen) was cocrystallized with 4-bromo-resorcinol and 3,5-dihydroxy-acetophenone (see structures a and b in Figure 7). In each case, resorcinol spacers and polyenes form discrete four-component molecular assemblies that are stabilized by four O−H···N hydrogen bonds, in which the templates orient the polyenes in a parallel arrangement. The separation between the stacked C═C bonds ranges from 3.82 to 3.85 Å (see Figure 7a) and 4.23 to 4.31 Å, respectively (see Figure 7b). Nearest-neighbor assemblies of each solid pack in an antiparallel fashion so that olefins of hydrogen-bonded assemblies are sole C═C bonds organized to undergo reaction. Though the dipyridines are arranged parallel to each other, they may not be suited for a photoreaction since the distance between the reactive double bond in a pair exceeds the threshold value of 4.2 Å for the photoreaction to occur. This particular adduct possesses an additional hydrogen-bonding acceptor C═O functional group, present on the spacer resorcinol, that is not involved in stabilizing the four-point molecular assemblies.

In addition, photoreactive conjugate dipyridine 1,4-bis[(*E*)-2-(4-pyridyl)ethenyl]-2-fluorobenzene (bpef) was cocrystallized with 4-bromo-resorcinol (see Figure 8a) and 2,4-dihydroxy-benzaldehyde (see Figure 8c). The presence of two fluorine atoms in Figure 8 is explained by an orientational disorder, i.e., the asymmetric molecule is built into the complex in two orientations with 50% occupation leading to the disorder. The supramolecular heterosynthon comprised of bpef and 4-bromo-

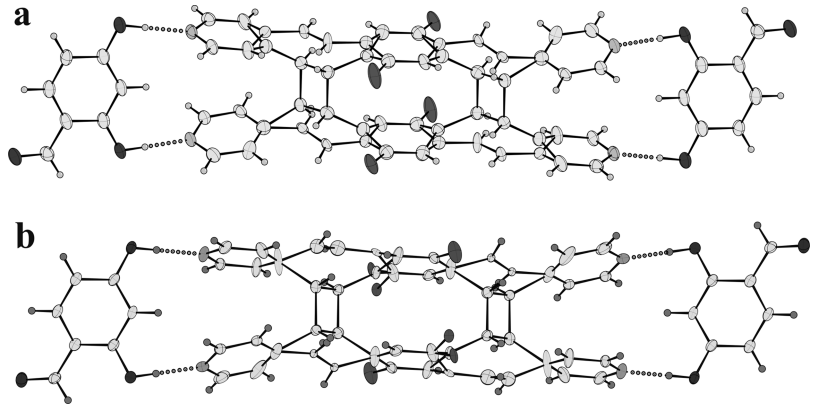

Figure 10. Projection of the crystal structures of mixed crystals obtained after short time (3 h) and long time irradiation (6 h): (a) ~40% converted mixed crystals, and (b) ~60% converted mixed crystals.

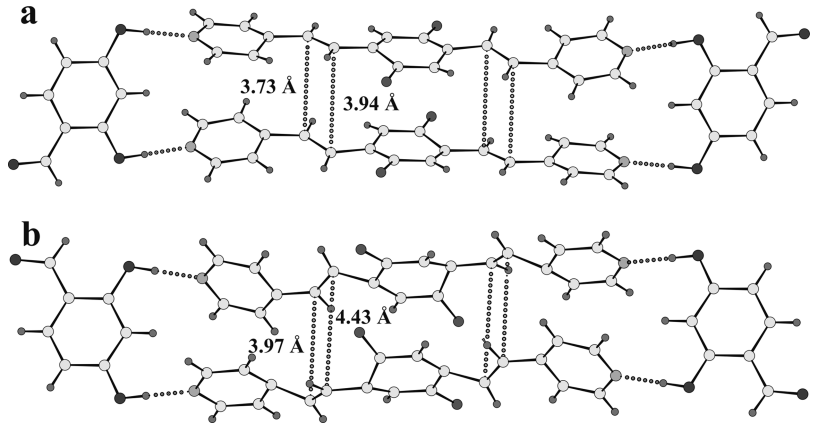

Figure 11. Projection of the crystal structures of the mixed crystals of complex bpef and 2,4-dihydroxy-benzaldehyde, where atoms belonging to the dimer have been omitted for clarity: (a) 40% conversion. (b) 60% conversion.

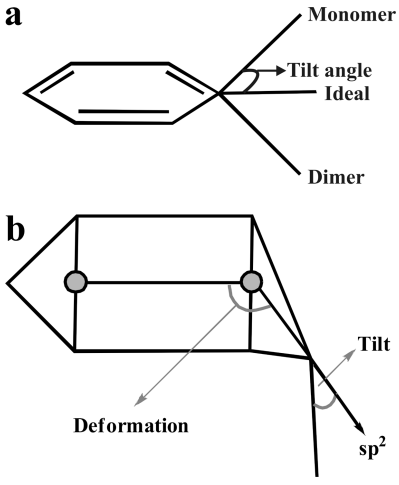

Figure 12. Schematic representation of (a) tilt angle and (b) ring deformation.

resorcinol (see Figure 8a) is one of the rather few examples of self-assembled photoreactive molecules in an anti-arrangement. Even though the complex has adopted a discrete 0D four point molecular recognition via the O−H···N heterosynthon with a double bond separation of less than 4.2 Å, it is not photoreactive, because the anti-arrangement of the molecules renders the reactive centers (double bond) perpendicular to each other contrary to the parallel orientation required for the photodimerization reaction to occur. From the projection of the crystal structure (seeFigure 8c), it is evident that the monomer complex of bpef and 2,4-dihydroxy-benzaldehyde has a rather perfect orientation, with two dipyridines lying approximately parallel to each other and separated by less than 3.8 Å, thus fulfilling the well-known geometry criteria of Schmidt for [2 + 2] photodimerizations.[17] This particular system is chosen for further analysis of reaction intermediates.

3.6. Monitoring Structural Changes by X-ray Analysis. A single-crystal-to-single-crystal[31,33] transformation was performed on crystals of bpef and 2,4-dihydroxy-benzaldehyde supramolecular heterosynthon, via tail irradiation with UV-light using a 458 nm filter (cf. Figure 9). Upon tail-irradiation, the crystals do not disintegrate but rather remain intact, hence facilitating single-crystal X-ray analysis of partially reacted crystals (mixed crystals). The projection of the crystal structure shown in Figure 10 corresponds to the short time (3 h, 40% converted, Figure 10a) and long time (6 h, 60% converted, Figure 10b) irradiated crystals. Mixed crystals are like a solid solution in which monomer and dimer molecules statistically occupy identical lattice sites. In these structures, separate atomic coordinates are observed for olefinic carbon atoms, the cyclobutane ring, and for those carbon atoms of the pyridyl and phenyl rings that are directly connected to the cyclobutane ring. All other atoms occupy identical positions as in the monomer complex (see Figure 8c), at least within the error of analysis. The population parameter (i. e., the level of conversion) was obtained from least-squares refinement.

Table 2. Tilt Angles for Substitutional Mixed Crystals of the Bpef Molecular Adduct at Different Conversions

Mixed Crystal Irradiated by	Tilt Angles	A	B	C	D	Structure
458nm Xe lamp 40%	Monomer:	10.6°	7.5°	3.9°	1.3°	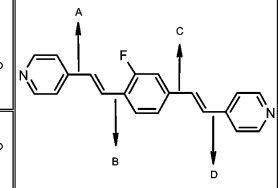
	Dimer:	22.2°	24.2°	24.7°	15.4°	
458nm Xe lamp 60%	Monomer:	15.4°	26.2°	3.7°	26.4°	
	Dimer :	16.5°	23.0°	20.0°	29.9°	

Table 3. Ring Deformation Angles for Substitutional Mixed Crystals of the Bpef Molecular Adduct

Mixed Crystal Irradiated by	Ring Deformation Angle A	B	C	D	Structure
458nm Xe lamp 40%	----	23.8°	23.2°	23.5°	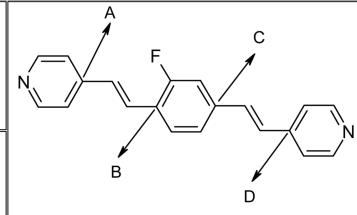
458nm Xe lamp 60%	----	27.6°	----	----	

A careful inspection of the corresponding structures revealed several interesting features. In contrast to changes observed during dimerization of cinnamic acid,[31a] where the side group atoms occupy the same lattice sites within the experimental error, some atoms belonging to the side groups split into monomer-associated and dimer-associated sites. These are the carbon atoms of pyridyl or phenyl rings, which are directly attached to the cyclobutane ring (or) to the vinylic carbon atoms. This effect can be explained by strain on the molecules present in the lattice of the mixed crystal of dimer and monomer. As shown in the Figure 8c, a distance of around 4 Å separates the monomer pair double bonds. The bond length in the cyclobutane ring is around 1.5 Å. These two moieties share one site in the crystal lattice, and as a consequence, both are distorted from their most favorable conformation.

A total conversion of 40% was achieved after 3 h of irradiation, whereas after 6 h the conversion had stopped (~60% conversion). Notably, the conversion did not continue even after long irradiation times, presumably because of changes of the distance between reacting centers. The distance between the reacting centers in the monomer before irradiation was 3.64 Å for the front carbon and 3.72 Å for the rear carbon, as shown in Figure 8c. After 40% conversion, this distance has changed to 3.73 and 3.94 Å and after 60% conversion, it had further increased to 3.97 and 4.43 Å for the front and rear carbon, respectively (see structures a and b in Figure 11). In these structures the atoms belonging to the dimer have been omitted to obtain a clear picture of the monomer distortion.

3.7. Tilting and Deformation of Pyridyl and Phenyl Rings. As previously reported,[31a] strain on molecules in the mixed crystals of partially dimerized cinnamic acid leads to a deformation called "tilt", e.g., the bond to the cyclobutane ring (or) residual double bond system is deformed out of its ideal sp^2 orientation, which is characterized by the tilt angle as defined

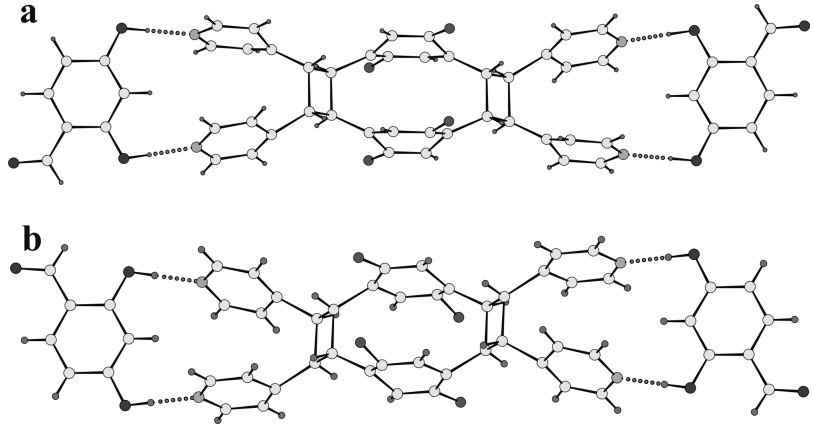

Figure 13. Projection of the crystal structure of mixed crystals of complex bpef and 2,4-dihydroxy-benzaldehyde, where atoms belonging to the monomer have been omitted for clarity, (a) short time (~40% converted) and (b) long time irradiation (60% converted).

schematically in Figure 12a. Tilt angles as large as 30° have been observed in the case of mixed crystals of partially dimerized molecular adduct of bpef and 2,4-dihydroxy-benzaldehyde (cf. Figure 8c). Table 2 gives the values of tilt angles obtained for both 40% and 60% converted mixed crystals of different moieties. It has been found that the tilt angle is mainly dependent on conversion, i.e., the minority component is always more tilted than the majority component. For example, the dimer, which is in minority in the 40% converted mixed crystals (see Figure 10a). is more tilted (22.2°) than the monomer, whereas in 60% converted mixed crystals (see Figure 10b), it is found to be less tilted (16.5°). The tilt deformation in mixed crystals of bpef is relieved by a distortion of pyridyl and phenyl rings, where the ring system bends so that it is no longer planar. The dimer, which is formed in this kind of cycloaddition, is a 2,2-cyclophane, [42] i.e., a compound where two *p*-phenylene groups are held face-to-face by $-[CH_2]-_2$ bridges. Generally, these kinds of deformations are characterized by a dihedral angle, which is schematically defined in Figure 12b. The deformations particularly found in partially dimerized bpef adducts are more severe than in cyclophanes, where deformation angles in the range of 15−16° on each side of the phenyl ring are observed. Dihedral angles obtained for different moieties in the bpef adduct are given in Table 3.

Tilt and deformation both are dependent on each other. If the deformation of the ring is larger, then the tilt angle is smaller; this helps in reducing the total strain on the molecule. The larger the tilt angle, the more the arm of the pyridyl rings is driven away from the reacting partner. This is clearly visible in the crystal structure projection shown in structures a and b in Figure 13 (atoms belonging to the monomer have been removed for clarity). As mentioned above, mixed crystals are like solid solutions where the dimer mimics the monomer at low conversion and the monomer mimic the dimer at rather high conversion. Therefore, the molecular deformation (tilt and ring deformation) of the monomer (which is in minority) in the 60% converted crystal (see Figure 11b) is much larger compared to the 40% converted crystals (see Figure 11a), where the monomer exists in majority and is thus less deformed. It should be noted that with increasing conversion, the distance between two reacting centers also increases, e.g., because of strain on the molecules, so that complete conversion cannot be accomplished in all cases.

4. Conclusions

In this report, an approach has been presented to achieve regiocontrol of [2 + 2] photoreactions supramolecularly in the solid state by using resorcinol as a spacer. The deliberate use of a variety of resorcinols containing competitive hydrogen-bonding active functional groups allowed us to determine the robust nature of the template. Major causes for a deviation of the design principle in case of hydroxyl−pyridine heterosynthons are, for example, undesired formation of intramolecular hydrogen bonds, the C−O bond flexibility of resorcinol, and steric hindrances. Moreover, X-ray analysis of intermediate states of the single-crystal-to-single-crystal transformation of 1,4-bis[(*E*)-2-(4-pyridyl)ethenyl]-2-fluorobenzene (bpef) with 2,4-dihydroxy-benzaldehyde allowed us to establish the topochemical nature of the photoreaction, as well as to analyze structural changes that occurred at a molecular level during the reaction.

Supporting Information Available: Crystal preparation table and more examples of OH···N recognition (PDF); crystal structures CIF files. This material is available free of charge via the Internet at http://pubs.acs.org.

References

(1) (a) Desiraju, G. R. *Angew. Chem., Int. Ed.* **1995**, *34*, 2311–2327. (b) Desiraju, G. R. *Nat. Mater.* **2002**, *1*, 77–79. (c) Desiraju, G. R. *Nature* **2001**, *412*, 397–400.
(2) Soldatov, D. V.; Terekhova, I. S. *J. Struct. Chem.* **2005**, *46*, S1–S8.
(3) Braga, D. *Chem. Commun.* **2003**, *22*, 2751–2754.
(4) Desiraju, G. R. *Chem. Commun.* **1997**, *16*, 1475–1482.
(5) Biradha, K. *CrystEngComm.* **2003**, *5*, 374–384.
(6) Cohen, M. D.; Schmidt, G. M. J. *J. Chem. Soc.* **1964**, 1996–2000.
(7) Cohen, M. D.; Schmidt, G. M. J.; Sonntag, F. I. *J. Chem. Soc.* **1964**, 2000–2013.
(8) Xiao, J.; Yang, M.; Lauher, J. W.; Flower, F. W. *Angew. Chem., Int. Ed.* **2000**, *39*, 2132–2135.
(9) Curtis, S. M.; Le, N.; Flower, F. W.; Lauher, J. W. *Cryst. Growth Des.* **2005**, *5*, 2313–2321.
(10) Fowler, F. W.; Lauher, J. W. *J. Phys. Org. Chem.* **2000**, *13*, 850–857.
(11) Schmidt, G. M. J. *Pure. Appl. Chem.* **1971**, *27*, 647–678.
(12) Ariel, S.; Askari, S.; Scheffer, J. R.; Trotter, J.; Walsh, L. *J. Am. Chem. Soc.* **1984**, *106*, 5726–5728.
(13) Murthy, G. S.; Arjunan, P.; Venkatesan, K.; Ramamurthy, V. *Tetrahedron* **1987**, *43*, 1225–1240.
(14) Aakeröy, C. B.; Seddon, K. R. *Chem. Soc. Rev.* **1993**, 397–407.
(15) Mac Donald, J.; Whitesides, G. M. *Chem. Rev.* **1994**, *94*, 2383–2420.
(16) (a) Liu, J.; Wandet, L. N.; Boarman, K. J. *Org. Lett.* **2005**, *7*, 1007–1010. (b) Vishnumurthy, K.; Guru Row, T. N.; Venkatesan, K. *Photochem. Photobiol. Sci.* **2002**, *1*, 427–430.
(17) Ramamurthy, V.; Venkatesan, K. *Chem. Rev.* **1987**, *87*, 433–481.
(18) Sharma, C. V. K.; Panneerselvam, K.; Shimoni, L.; Katz, H.; Karell, H. L.; Desiraju, G. R. *Chem. Mater.* **1994**, *6*, 1282–1292.
(19) Feldman, K. S.; Campbell, R. F. *J. Org. Chem.* **1995**, *60*, 1924–1925.
(20) (a) MacGillivary, L. R.; Reid, J. L.; Ripmeester, J. A. *J. Am. Chem. Soc.* **2000**, *122*, 7817–7818. (b) Papefstathiou, G. S.; Kipp, A. J.; MacGillivray, L. R. *Chem. Commun.* **2001**, 2462–2463. (c) Varshney, D. B.; Papefstathiou, G. S.; MacGillivray, L. R. *Chem. Commun.* **2002**, 1964–1965. (d) Friscic, T.; Drab, D. M.; MacGillivray, L. R. *Org., Lett.* **2004**, *6*, 4647–4650. (e) Friscic, T.; MacGillivray, L. R. *Chem. Commun.* **2005**, 5748–5750.
(21) Moulton, B.; Zaworotko, M. J. *Chem. Rev.* **2001**, *101*, 1629–1658.
(22) MacGillivray, L. R.; Atwood, J. L. *J. Am. Chem. Soc.* **1997**, *119*, 6931–6932.
(23) (a) Bucar, D. K.; Henry, R. F.; Lou, X.; Durest, R. W.; Borchardt, T. B.; MacGillivray, L. R.; Geoff, G.; Zhang, Z. *Mol. Pharm.* **2007**, *4*, 339–346. (b) Bis, J. A.; Vishweshwar, P.; Weyna, D.; Zaworotko, M. J. *Mol. Pharm.* **2007**, *3*, 401–416. (c) Bis, J. A.; Zaworotko, M. J. *Cryst. Growth Des.* **2005**, *5*, 1169–1197. (d) Zhang, J.; Wu, L.; Fan, Y. *J. Mol. Struct.* **2003**, *660*, 119–129.
(24) Walsh, R. D. B.; Bradner, M. W.; Fleishman, S.; Morales, L. A.; Moulton, B.; Rodrigues-Hornedo, N.; Zaworotko, M. J. *Chem. Commun.* **2003**, *2*, 186–187.
(25) Vangla, V. R.; Mondal, R.; Broder, C. K.; Howard, J. A. K.; Desiraju, G. R. *Cryst. Growth Des.* **2005**, *5*, 99–104.
(26) (a) Steiner, T. *Acta. Crystallogr., Sect. B* **2001**, *57*, 103–106. (b) Vishweshwar, P.; Nangia, A.; Lynch, V. M. *J. Org. Chem.* **2002**, *67*, 556–565. (c) Aakeroy, C. B.; Beatty, A. M.; Helfrich, B. A. *J. Am. Chem. Soc.* **2002**, *124*, 14425–14432.
(27) Vishweshwar, P.; Nangia, A.; Lynch, V. M. *Cryst. Growth Des.* **2003**, *3*, 783–790.
(28) Papaefsthathiou, G. S.; Macgillivary, L. R. *Org. Lett.* **2001**, *3*, 3835–3838.
(29) Kaupp, G. *Angew. Chem., Int. Ed.* **1992**, *31*, 592–595.
(30) (a) Atkinson, S. D. M.; Almond, M. J.; Bowmaker, G. A.; Drew, M. G. B.; Feltham, E. J.; Hollins, P.; Jenkins, S. L.; Wiltshire, K. S. *J. Chem. Soc., Perkin Trans. 2* **2002**, *9*, 1533–1537. (b) Davaasambuu, J.; Busse, G.; Techert, S. *J. Phys. Chem. A* **2006**, *110*, 3261–3265.
(31) (a) Enkelmann, V.; Wegner, G.; Novak, K. *J. Am. Chem. Soc.* **1993**, *115*, 10390–10391. (b) Abdelmoty, I.; Buchholz, V.; Di, L.; Enkelmann, V.; Wegner, G.; Foxman, M. *Cryst. Growth. Des.* **2005**, *17*, 2210–2217. (c) Khan, M.; Enkelmann, V.; Brunklaus, G. *CrystEngComm.* **2009**, doi: 10.1039/b820732a.
(32) (a) Khan, M.; Brunklaus, G.; Enkelmann, V.; Spiess, H. W. *J. Am. Chem. Soc.* **2008**, *130*, 1741–1748. (b) Khan, M.; Enkelmann, V.; Brunklaus, G. *J. Org. Chem.* **2009**, *74*, 2261–2270.

(33) Friscis, T.; MacGillivray, L. R. *Z. Kristallogr.* **2005**, 351–363.
(34) Vatsadze, S. Z.; Nuriev, V. N.; Chernikov, A. V.; Zyk, N. V. *Russ. Chem. Bull.* **2002**, *51*, 1957–1958.
(35) Leiserowitz, L.; Hagler, A.; T. *Proc. R. Soc. London* **1983**, *A388*, 133–175.
(36) (a) Etter, M. C. *Acc. Chem. Res.* **1990**, *23*, 120–126. (b) Etter, M. C.; Urbanczyk-Lipkowska, Z.; Zia-Ebrahimi, M.; Panunto, T. W. *J. Am. Chem. Soc.* **1990**, *112*, 8415–8426.
(37) Etter, M. C. *J. Phys. Chem.* **1991**, *95*, 4601–4610.
(38) Nguyen, T. L.; Scott, A.; Dinkelmeyer, B.; Fowler, F. W.; Lauher, J. W. *New J. Chem.* **1998**, 129–135.
(39) (a) Couper, P. I.; Ferguson, G.; Glidewell, C. *Acta Crystallogr., Sect. C* **1996**, *52*, 2524–2528. (b) Wheatley, P. S.; Lough, A. J.; Ferguson, G.; Glidewell, C. *Acta. Crystallogr., Sect. C* **1999**, *55*, 1489–1492.
(40) (a) MacGillivray, L. R. *J. Org. Chem.* **2008**, *73*, 3311–3317. (b) MacGillivray, L. R.; Papaefstathiou, G. S.; Friscic, T.; Hamilton, D.; Bucar, D. K.; Chu, Q.; Varshney, D. B.; Georgiev, I. G. *Acc. Chem. Res.* **2008**, *41*, 280–291.
(41) Allen, F. H. *Acta Crystallogr., Sect. B* **2002**, *58*, 380–388.
(42) Bickelhaupt, F. *Pure Appl. Chem.* **1990**, *62*, 373–382.

CG801249B